American Journal of Engineering Research (AJER)
e-ISSN : 2320-0847 p-ISSN : 2320-0936
Volume-02, Issue-11, pp-48-60
www.ajer.org

Research Paper Open Access

Improvement of Transient stability in Power Systems with Neuro-Fuzzy UPFC

Gundala Srinivasa Rao, Venugopal Reddy Bodha

Abstract: - Low Frequency Oscillations (LFO) occur in power systems because of lack of the damping torque in order to dominance to power system disturbances as an example of change in mechanical input power. In the recent past Power System Stabilizer (PSS) was used to damp LFO. FACTs devices, such as Unified Power Flow Controller (UPFC), can control power flow, reduce sub-synchronous resonance and increase transient stability. So UPFC may be used to damp LFO instead of PSS. UPFC damps LFO through direct control of voltage and power. In this paper the linearized model of synchronous machine (Heffron-Philips) connected to infinite bus (Single Machine-Infinite Bus: SMIB) with UPFC is used and also in order to damp LFO, adaptive neuro-fuzzy controller for UPFC is designed and simulated. Simulation is performed for various types of loads and for different disturbances. Simulation results show good performance of neuro-fuzzy controller in damping LFO.

Keywords: - *Neuro-Fuzzy Controller, Low Frequency Oscillations (LFO), Unified Power Flow Controller (UPFC), Single Machine-Infinite Bus (SMIB)*

I. INTRODUCTION

The Benefits of Flexible AC Transmission Systems (FACTs) usage to improve power systems stability is well known. The growth of the demand for electrical energy leads to loading the transmission system near their limits. Thus, the occurrence of the LFO has increased. FACTs Controllers has capability to control network conditions quickly and this feature of FACTs can be used to improve power system stability. The UPFC is a FACTS device that can be used to the LFO. The primarily use of UPFC is to control the power flow in power systems. The UPFC consists of two voltage source converters (VSC) each of them has two control parameters namely m_e, δ_e, m_b and δ_b. The UPFC used for power flow control, enhancement of transient stability, mitigation of system oscillations and voltage regulation. For systems which are without power system stabilizer (PSS), excellent damping can be achieved via proper controller design for UPFC parameters. By designing a suitable UPFC controller, an effective damping can be achieved. It is usual that Heffron-Philips model is used in power system to study small signal stability. This model has been used for many years providing reliable results.
In recent years, the study of UPFC control methods has attracted attentions so that different control approaches are presented for UPFC control such as Fuzzy control, conventional lead-lag control, Genetic algorithm approach, and robust control methods.

In this study, the class of adaptive networks that of the same as fuzzy inference system in terms of performance is used. The controller utilized with the above structure is called Adaptive Neuro Fuzzy Inference System or briefly ANFIS. Applying neural networks has many advantages such as the ability of adapting to changes, fault tolerance capability, recovery capability, High-speed processing because of parallel processing and ability to build a DSP chip with VLSI Technology. To show performance of the designed adaptive neuro-fuzzy controller, a conventional lead-lag controller that is used and the simulation results for the power system including these two controllers are compared with each other.

II. FLEXIBLE AC TRANSMISSION SYSTEMS (FACTS)

Flexible AC Transmission Systems, called FACTS, got in the recent years a well known term for higher controllability in power systems by means of power electronic devices. Several FACTS-devices have been introduced for various applications worldwide. A number of new types of devices are in the stage of being introduced in practice.

In most of the applications the controllability is used to avoid cost intensive or landscape requiring extensions of power systems, for instance like upgrades or additions of substations and power lines. FACTS-devices provide a better adaptation to varying operational conditions and improve the usage of existing installations. The basic applications of FACTS-devices are:

Power flow control, Increase of transmission capability, Voltage control, Reactive power compensation, Stability improvement, Power quality improvement, Power conditioning, Flicker mitigation, Interconnection of renewable and distributed generation and storages.

The development of FACTS-devices has started with the growing capabilities of power electronic components. Devices for high power levels have been made available in converters for high and even highest voltage levels.

The overall starting points are network elements influencing the reactive power or the impedance of a part of the power system. Figure 1.2 shows a number of basic devices separated into the conventional ones and the FACTS-devices.

For the FACTS side the taxonomy in terms of 'dynamic' and 'static' needs some explanation. The term 'dynamic' is used to express the fast controllability of FACTS-devices provided by the power electronics. This is one of the main differentiation factors from the conventional devices. The term 'static' means that the devices have no moving parts like mechanical switches to perform the dynamic controllability. Therefore most of the FACTS-devices can equally be static and dynamic.

The left column in Figure.1 contains the conventional devices build out of fixed or mechanically switch able components like resistance, inductance or capacitance together with transformers. The FACTS-devices contain these elements as well but use additional power electronic valves or converters to switch the elements in smaller steps or with switching patterns within a cycle of the alternating current. The left column of FACTS-devices uses Thyristor valves or converters. These valves or converters are well known since several years. They have low losses because of their low switching frequency of once a cycle in the converters or the usage of the Thyristors to simply bridge impedances in the valves.

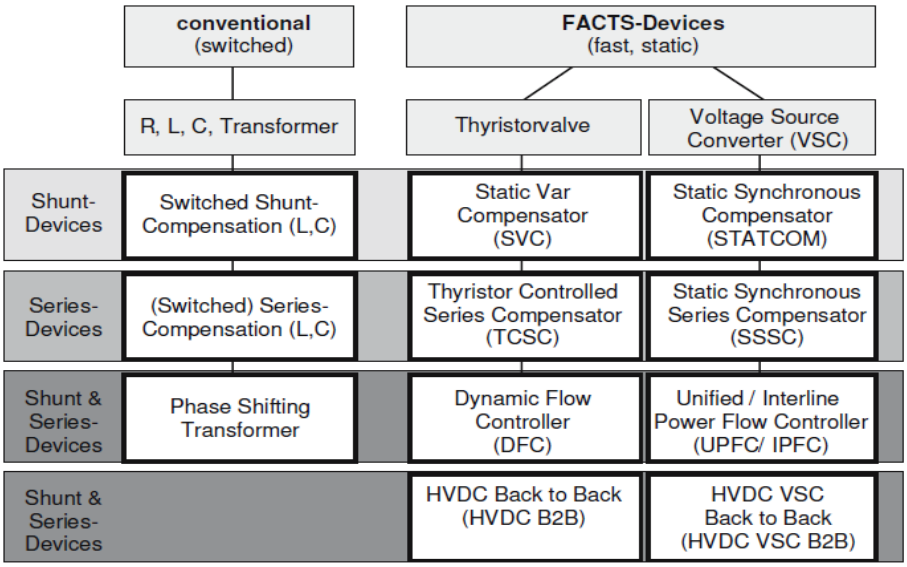

Fig.1. Overview of FACTS Devices

The right column of FACTS-devices contains more advanced technology of voltage source converters based today mainly on Insulated Gate Bipolar Transistors (IGBT) or Insulated Gate Commutated Thyristors (IGCT). Voltage Source Converters provide a free controllable voltage in magnitude and phase due to a pulse width modulation of the IGBTs or IGCTs.

High modulation frequencies allow to get low harmonics in the output signal and even to compensate disturbances coming from the network. The disadvantage is that with an increasing switching frequency, the losses are increasing as well. Therefore special designs of the converters are required to compensate this.

III. UNIFIED POWER FLOW CONTROLLER

The UPFC is a combination of a static compensator and static series compensation. It acts as a shunt compensating and a phase shifting device simultaneously.

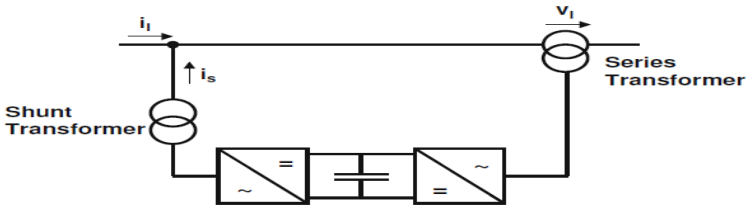

Fig.2. Principle configuration of an UPFC

The UPFC consists of a shunt and a series transformer, which are connected via two voltage source converters with a common DC-capacitor.
The DC-circuit allows the active power exchange between shunt and series transformer to control the phase shift of the series voltage. This setup, as shown in Figure 1.21, provides the full controllability for voltage and power flow.
The series converter needs to be protected with a Thyristor bridge. Due to the high efforts for the Voltage Source Converters and the protection, an UPFC is getting quite expensive, which limits the practical applications where the voltage and power flow control is required simultaneously.

Circuit Arrangement:

In the presently used practical implementation, The UPFC consists of two switching converters, which in the implementations considered are voltage source inverters using gate turn-off (GTO) thyristor valves, as illustrated in the Fig.3. These back to back converters labeled "Inverter 1 and "Inverter 2" in the figure are operated from a common dc link provided by a dc storage capacitor.
This arrangement functions as an ac to ac power converter in which the real power can freely flow in either direction between the ac terminals of the two inverters and each inverter can independently generate (or absorb) reactive power at its own ac output terminal.

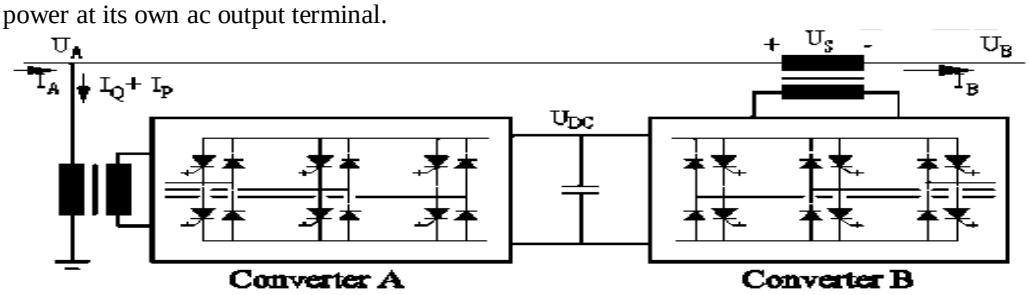

Fig.3. Basic circuit arrangement of unified power flow controller

Operation of UPFC:

Inverter 2 provides the main function of the UPFC by injecting an ac voltage Vpq with controllable magnitude V_{pq} ($0 \le V_{pq} \le V_{pqmax}$) and phase angle $\rho(0 \le \rho \le 360)$, at the power frequency, in series with the line via an insertion transformer. The injected voltage is considered essentially as a synchronous voltage source. The transmission line current flows through this voltage source resulting in real and reactive power exchange between it and the ac system. The real power exchanged at the ac terminal (i.e., at the terminal of insertion transformer) is converted by the inverter into dc power that appears at the dc link as positive or negative real power demanded. The reactive power exchanged at the ac terminal is generated internally by the inverter.

The basic function of inverter 1 is to supply or absorb the real power demanded by Inverter 2 at the common dc link. This dc link power is converted back to ac and coupled to the transmission line via a shunt-connected transformer. Inverter 1 can also generate or absorb controllable reactive power, if it is desired, and there by it can provide independent shunt reactive compensation for the line.

It is important to note that where as there is a closed "direct" path for the real power negotiated by the action of series voltage injection through Inverters 1 and 2 back to the line, the corresponding reactive power exchanged is supplied or absorbed locally by inverter 2 and therefore it does not flow through the line.
Thus, Inverter 1 can be operated at a unity power factor or be controlled to have a reactive power exchange with the line independently of the reactive power exchanged by the Inverter 2. This means there is no continuous reactive power flow through UPFC.

Basic Control Functions:

Operation of the UPFC from the standpoint of conventional power transmission based on reactive shunt compensation, series compensation, and phase shifting, the UPFC can fulfill these functions and thereby

meet multiple control objectives by adding the injected voltage V_{pq}, with appropriate amplitude. And phase angle, to the terminal voltage V_o. Using phasor representation, the basic UPFC power flow control functions are illustrated in Fig 4.

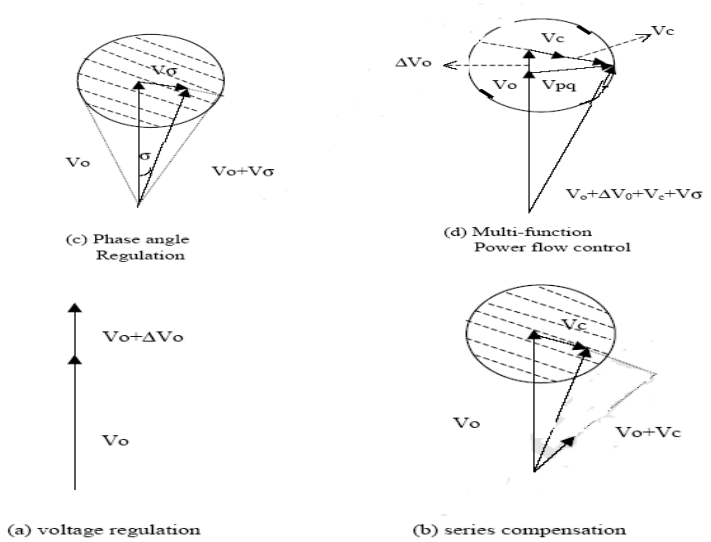

Fig.4. Basic UPFC control functions

Terminal Voltage Regulation, similar to that obtainable with a transformer tap-changer having infinitely small steps, as shown at (a) where $V_{pq}=\Delta V$ (boldface letters represent phasors) is injected in-phase (or anti-phase) with V_o.

Series capacitor compensation is shown at (b) where $V_{pq}=V_c$ is in quadrature with the line current I.

Transmission angle Regulation (phase shifting) is shown at (c) where $V_{pq}=V_o$ is injected with angular relationship with respect to V_o that achieves the desired s phase shift (advance or retard) without any change in magnitude.

Multifunctional Power Flow Control, executed by simultaneous terminal voltage regulation, series capacitive compensation, and phase shifting, is shown at (d) where $V_{pq}=\Delta V+V_c+V_o$.

Basic Principles Of P And Q Control:

Consider Fig 2.3. At (a) a simple two machine (or two bus ac inter-tie) system with sending end voltage V_s, receiving-end voltage V_r, and line (or tie) impedance X (assumed, for simplicity, inductive) is shown. At (b) the voltages of the system in the form of a phasor diagram are shown with transmission angle δ and $|V_s|=|V_r|=V$. At (c) the transmitted power P ($P=V_2/X \sin\delta$) and the reactive power $Q=Q_s=Q_r$ ($Q=V_2/X\ (1-\cos\delta)$) supplied at the ends of the line are shown plotted against angle δ. At (d) the reactive power $Q=Q_s=Q_r$ is shown plotted against the transmitted power corresponding to "stable values of δ" (i.e., $0<=\delta<=90^o$).

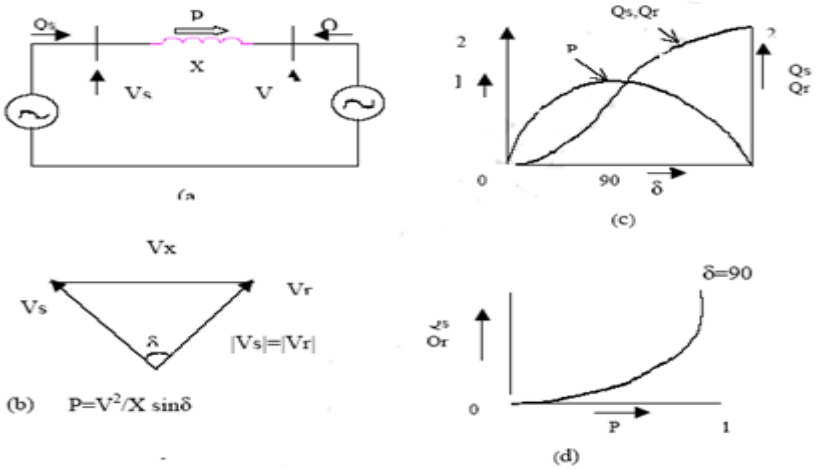

Fig.5. simple two machine system (a) related voltage phasor (b).real and reactive power verses transmission angle (c). and sending-end/receiving-end reactive power verses transmitted real power(d).

Basic power system of fig.5 with the well known transmission characteristics is introduced for the purpose of providing a vehicle to establish the capability of the UPFC to control the transmitted real power P and the reactive power demands, Q_s and Q_r, at the sending end, respectively, the receiving end of the line.
The UPFC is represented by a controllable voltage source in series with the line which, as explained in the previous section, can generate or absorb reactive power that it, or absorbed from it, bye the sending end generator.

The UPFC in series with the line is represented by the phasor V_{pq} having magnitude $V_{pq}(0 \leq V_{pq} \leq V_{pqmax})$ and angle ρ $(0 \leq \rho \leq 360)$ measured from the given phase position of phasor Vs, as illustrated in the figure. The line current represented by the phasor I, flows through the series voltage source, V_{pq} and generally results in both reactive and real power exchange. In order to represent UPFC properly, the series voltage source is stipulated to generate only the reactive power Q_{pq} it exchanges with the line. Thus the real power P_{pq} it negotiates with the line is assumed to be transferred to the sending-end generator excited.
This is in arrangement with the UPFC circuit structure in which the dc link between the two constituent inverters establish a bi-directional coupling for real power flow between the injected series voltage source and the sending end bus.

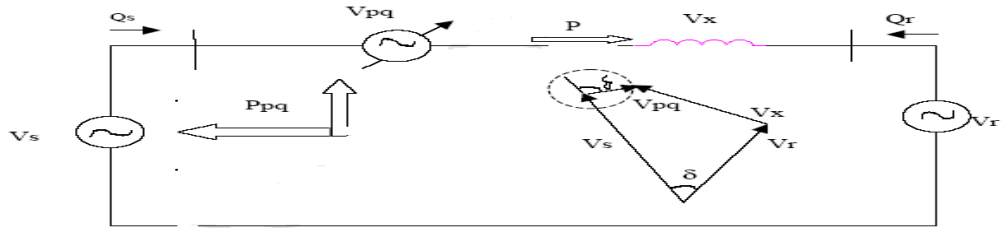

It can be observed in Fig that the transmission line "sees" V_s+V_{pq} as the effective sending end voltage. Thus it is clear that the UPFC effects the voltage (both its magnitude and angle) across the transmission line and therefore it is reasonable to expect that it is able to control, by varying the magnitude and angle of Vpq, the transmittable real power as well as the reactive power demand of the line at any given transmission angle between the sending-end and receiving-end voltages.

Independent Real And Reactive Power Flow Control:

In Fig2.5(a) through 2.5(b) the reactive power Q_s supplied by the sending-end generator, and Q_r supplied by the receiving-end generator, are shown plotted separately against the transmitted power ρ as a function of the magnitude Vpq and angle p of the injected voltage phasor V_{pq} at four transmission lines; δ=0,30,60 and 90. At V_{pq}=0 each of these plots becomes a discrete point on the basic Q-p curve as shown in Fig 2.3(d), which is included in each of the above figures for reference.
The curves showing the relationships between Q_s and P, and Q_r and P, for the transmission angle range of 0<= δ<=90, when the UPFC is operated to provide the maximum transmittable power with no reactive power control ($V_{pq}=V_{pqmax}$ and ρ= ρp=P_{max}), are also shown by a broken –line with the label "P (δ) =MAX" at the sending end and respectively, "receiving-end" plots of the figure.

Consider the first fig.5 (a), which illustrates the case when the transmission angle is zero(δ=0). With V_{pq}=0, P, Qs and Q_r are all zero, i.e., the system is standstill at the origins of the Q_s, P and Q_r, P coordinates. The circle around the origin of the {Q_s, P} and {Qr, P} planes sown the variation of Q_s and P and Q_r and P respectively. As the voltage phasor Vpq, with its maximum V_{pqmax} is rotated a full revolution (0<= ρ<=360). The area within these circles defines all P and Q values obtainable by controlling the magnitude V_{pq} and ρ of the phasor V_{pq}.

In other words, the circle in {Q_s,p} and {Q_r,p} planes define all P and Qs and respectively, P and Q_r values attainable with the UPFC of a given rating. It can be observed, for example, that the UPFC with the stipulated voltage rating of 0.5. P.u. is able to establish 0.5. P.u. power flow, in either direction, without imposing any reactive power demand on either the sending-end or the receiving-end generator.
Of course, the UPFC, as seen, can force the generator at one end to supply reactive power for the generator at the other end. (In case of inertia, one system can be forced to supply reactive power of the line.)

In general at any given transmission angle δ, the transmitted real power P, and the reactive power demands at the transmission line ends, Q_s and Q_r, can be controlled freely by the UPFC within the boundaries obtained in the {Qs,p}and {Q_r,P} planes by rotating the injected voltage phasor V_{pq} with its maximum magnitude a full revolution. The boundary in each plane is centered around the point defined by the transmission angle on the Q verses P curve that characteristic the basic power transmission at V_{pq}=0.

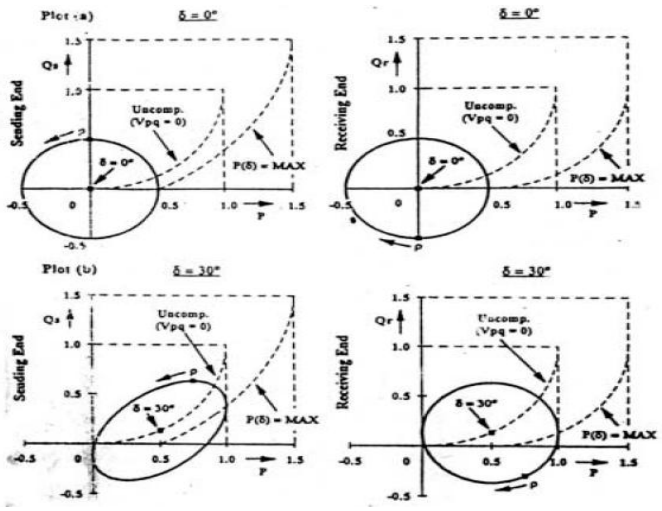

Fig.6. Attainable sending-end reactive power Vs transmitted power (left hand side plots) and receiving-end reactive power Vs transmitted power (right hand side plots) values with the UPFC at $\delta=0^o$ and $\delta=30^o$

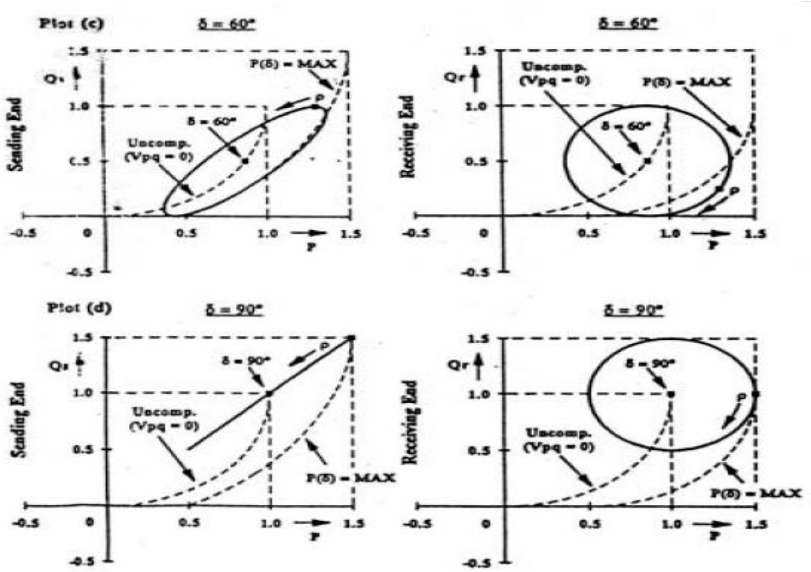

Fig .7. Attainable sending-end reactive power Vs transmitted power (left-hand side plots) and receiving-end reactive power Vs transmitted power (right hand side plots) values with the UPFC at $\delta=60^o$ and $\delta=90^o$

Consider the next case of δ=30, it is seen that the receiving-end control region boundary in the {Q_s, P} plane become an ellipse. As the transmission angle δ is further increased, for example, to 60 , the ellipse defining the control region for P and Qs in the {Q_s, P} plane becomes narrower and finally 90 it degerates into a straight line. By contrast, the control region boundary for p and Q_r in the {Q_r,P} plane remains a circle at all transmission angles.

DAMPING OSCILLATIONS OF UPFC:

Problem Statement:

Figure8 shows a SMIB system equipped with a UPFC. The UPFC consists of an excitation transformer (ET), a boosting transformer (BT), two three-phase GTO based voltage source converters (VSCs), and a DC link capacitors. The four input control signals to the UPFC are m_E, m_B, δ_E, and δ_B, where

m_E is the excitation amplitude modulation ratio,

m_B is the boosting amplitude modulation ratio,

δ_E is the excitation phase angle, and

δ_B is the boosting phase angle.

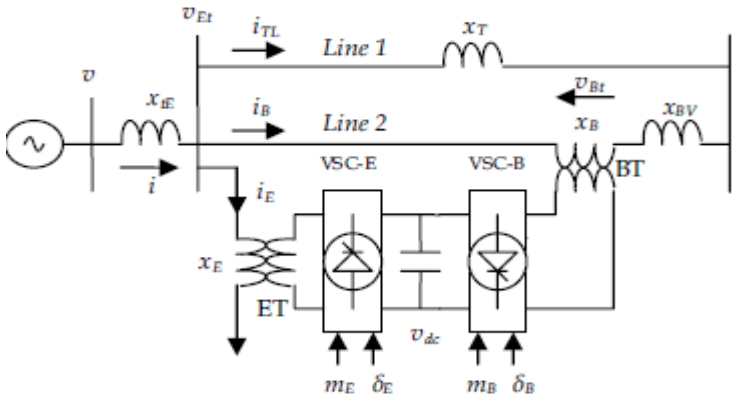

Fig.8. SMIB power system equipped with UPFC

Power System Nonlinear Model:

By applying Park's transformation and neglecting the resistance and transients of the ET and BT transformers, the UPFC can be modeled as

$$\begin{bmatrix} v_{Etd} \\ v_{Etq} \end{bmatrix} = \begin{bmatrix} 0 & -x_E \\ x_E & 0 \end{bmatrix} \begin{bmatrix} i_{Ed} \\ i_{Eq} \end{bmatrix} + \begin{bmatrix} \frac{m_E \cos\delta_E v_{dc}}{2} \\ \frac{m_E \sin\delta_E v_{dc}}{2} \end{bmatrix} \quad (1)$$

$$\begin{bmatrix} v_{Btd} \\ v_{Btq} \end{bmatrix} = \begin{bmatrix} 0 & -x_B \\ x_B & 0 \end{bmatrix} \begin{bmatrix} i_{Bd} \\ i_{Bq} \end{bmatrix} + \begin{bmatrix} \frac{m_B \cos\delta_B v_{dc}}{2} \\ \frac{m_B \sin\delta_B v_{dc}}{2} \end{bmatrix} \quad (2)$$

$$\dot{v}_{dc} = \frac{3m_E}{4C_{dc}} \begin{bmatrix} \cos\delta_E & \sin\delta_E \end{bmatrix} \begin{bmatrix} i_{Ed} \\ i_{Eq} \end{bmatrix} + \frac{3m_B}{4C_{dc}} \begin{bmatrix} \cos\delta_B & \sin\delta_B \end{bmatrix} \begin{bmatrix} i_{Bd} \\ i_{Bq} \end{bmatrix} \quad (3)$$

Where v_{Et}, i_E, v_{Bt}, and i_B are the excitation voltage, excitation current, boosting voltage, and boosting current, respectively; C_{dc} and v_{dc} are the DC link capacitance and voltage, respectively.

The ET, BT and line 2 currents can be stated as:

$$i_{TLd} = \frac{1}{x_T}(x_E i_{Ed} + \frac{m_E \sin\delta_E v_{dc}}{2} - v_b \cos\delta) \quad (4)$$

$$i_{TLq} = \frac{1}{x_T}(x_E i_{Eq} - \frac{m_E \cos\delta_E v_{dc}}{2} + v_b \sin\delta) \quad (5)$$

$$i_{Ed} = \frac{x_{BB}}{x_{d2}} E'_q + x_{d7} \frac{m_B \sin\delta_B v_{dc}}{2} + x_{d5} v_b \cos\delta + x_{d6} \frac{m_E \sin\delta_E v_{dc}}{2} \quad (6)$$

$$i_{Eq} = x_{q7} \frac{m_B \cos\delta_B v_{dc}}{2} + x_{q5} v_b \sin\delta + x_{q6} \frac{m_E \cos\delta_E v_{dc}}{2} \quad (7)$$

$$i_{Bd} = \frac{x_E}{x_{d2}} E'_q - \frac{x_{d1}}{x_{d2}} \frac{m_B \sin\delta_B v_{dc}}{2} + x_{d3} v_b \cos\delta + x_{d4} \frac{m_E \sin\delta_E v_{dc}}{2} \quad (8)$$

$$i_{Bd} = \frac{x_{q1}}{x_{q2}} \frac{m_B \cos\delta_B v_{dc}}{2} + x_{q3} v_b \sin\delta + x_{q4} \frac{m_E \cos\delta_E v_{dc}}{2} \quad (9)$$

Where x_E and x_B are the ET and BT reactance, respectively; the reactances x_{qE}, x_{dE}, x_{BB}, x_{d1}-x_{d7}, and x_{q1}- x_{q7} are as shown in

The non-linear model of the SMIB system of Figure 1 is:

$$\dot{\delta} = \omega_b(\omega - 1) \quad (10)$$

$$\dot{\omega} = (P_m - P_e - D(\omega - 1))/M \quad (11)$$

$$\dot{E}'_q = (E_{fd} - (x_d - x'_d)i_d - E'_q)/T'_{do} \quad (12)$$

$$\dot{E}_{fd} = (K_A(V_{ref} - v + u_{PSS}) - E_{fd})/T_A \quad (13)$$

Where $P_e = v_d i_d + v_q i_q, v = (v_d^2 + v_q^2)^{1/2}, v_d = x_q i_q,\ v_q = E'_q - x'_d i_d, i_d = i_{Ed} + i_{Bd}, i_q = i_{Eq} + i_{Bq}$

P_m and P_e are the input and output power, respectively; M and D the inertia constant and damping coefficient, respectively; ω_b the synchronous speed; δ and ω the rotor angle and speed, respectively; E_q', E'_{fd}, and v the generator internal, field and terminal voltages, respectively; T'_{do} the open circuit field time constant; x_d, x'_d, and x_q the d-axis reactance, d-axis transient reactance, and q-axis reactance, respectively; KA and TA the exciter gain and time constant, respectively; V_{ref} the reference voltage; and u_{PSS} the PSS control signal.

Power System Linearized Model:

The non-linear dynamic equations can be linearized around a given operating point to have the linear model given by:

$$\dot{x} = Ax + Bu \quad (14)$$

Where the state vector x, control vector u, and matrices A and B are

$$x = \begin{bmatrix} \Delta\delta & \Delta\omega & \Delta E'_q & \Delta E_{fd} & \Delta v_{dc} \end{bmatrix}^T \quad (15)$$

$$u = \begin{bmatrix} \Delta u_{pss} & \Delta m_E & \Delta\delta_E & \Delta m_b & \Delta\delta_b \end{bmatrix}^T \quad (16)$$

$$A = \begin{bmatrix} 0 & \omega_b & 0 & 0 & 0 \\ -\frac{K_1}{M} & -\frac{D}{M} & -\frac{K_2}{M} & 0 & -\frac{K_{pd}}{M} \\ -\frac{K_4}{T'_{do}} & 0 & -\frac{K_3}{T'_{do}} & \frac{1}{T'_{do}} & -\frac{K_{qd}}{T'_{do}} \\ -\frac{K_A K_5}{T_A} & 0 & -\frac{K_A K_6}{T_A} & -\frac{1}{T_A} & -\frac{K_A K_{vd}}{T_A} \\ K_7 & 0 & K_8 & 0 & -K_9 \end{bmatrix} \quad (17)$$

$$B = \begin{bmatrix} 0 & 0 & 0 & 0 & 0 \\ 0 & -\frac{K_{pe}}{M} & -\frac{K_{p\delta e}}{M} & -\frac{K_{pb}}{M} & -\frac{K_{p\delta b}}{M} \\ 0 & -\frac{K_{qe}}{T'_{do}} & -\frac{K_{q\delta e}}{T'_{do}} & -\frac{K_{qb}}{T'_{do}} & -\frac{K_{q\delta b}}{T'_{do}} \\ \frac{K_A}{T_A} & -\frac{K_A K_{ve}}{T_A} & -\frac{K_A K_{v\delta e}}{T_A} & -\frac{K_A K_{vb}}{T_A} & -\frac{K_A K_{v\delta b}}{T_A} \\ 0 & K_{ce} & K_{c\delta e} & K_{cb} & K_{c\delta b} \end{bmatrix} \quad (18)$$

Where $K_1 - K_9$, K_{pu}, K_{qu}, and K_{vu} are linearization constants.

***Model Of The Power System Including* UPFC:**

UPFC is one of the famous FACTs devices that is used to improve power system stability. Fig.1 shows a single machine-infinite-bus (SMIB) system with UPFC. It is assumed that the UPFC performance is based on pulse width modulation (PWM) converters. In figure 1 m_e, m_b and δ_e, δ_b are the amplitude modulation ratio and phase angle of the reference voltage of each voltage source converter respectively. These values are the input control signals of the UPFC.

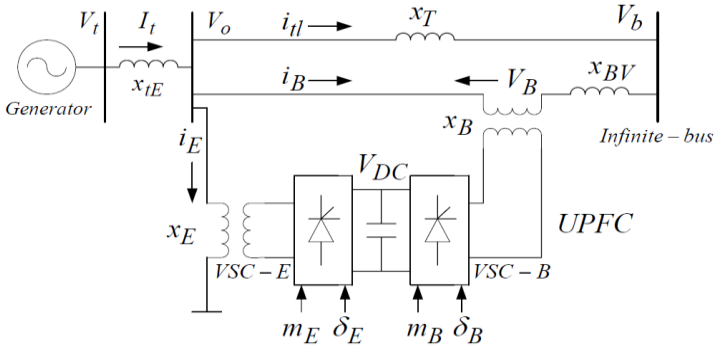

Fig.1 A single machine connected to infinite bus with UPFC

As it mentioned previously, a linearized model of the power system is used in dynamic studies of power system. In order to consider the effect of UPFC in damping of LFO, the dynamic model of the UPFC is employed; In this model the resistance and transient of the transformers of the UPFC can be ignored. The Linearized state variable equations of the power system equipped with the UPFC can be represented as

$$\begin{bmatrix} \Delta\dot{\delta} \\ \Delta\dot{\omega} \\ \Delta\dot{E}'_q \\ \Delta\dot{E}_{fd} \\ \Delta\dot{v}_{dc} \end{bmatrix} = \begin{bmatrix} 0 & \omega_0 & 0 & 0 & 0 \\ -\frac{k_1}{M} & -\frac{D}{M} & -\frac{k_2}{M} & 0 & -\frac{k_{pd}}{M} \\ -\frac{k_4}{T'_{do}} & 0 & -\frac{k_3}{T'_{do}} & \frac{1}{T'_{do}} & \frac{k_{qd}}{T'_{do}} \\ -\frac{k_A k_5}{T_A} & 0 & -\frac{k_A k_6}{T_A} & -\frac{1}{T_A} & -\frac{k_A k_{vd}}{T_A} \\ k_7 & 0 & k_8 & 0 & -k_9 \end{bmatrix} \begin{bmatrix} \Delta\delta \\ \Delta\omega \\ \Delta E'_q \\ \Delta E_{fd} \\ \Delta v_{dc} \end{bmatrix} + \begin{bmatrix} 0 & 0 & 0 & 0 \\ -\frac{k_{pe}}{M} & -\frac{k_{p\delta e}}{M} & -\frac{k_{pb}}{M} & -\frac{k_{p\delta b}}{M} \\ -\frac{k_{qe}}{T'_{do}} & -\frac{k_{q\delta e}}{T'_{do}} & -\frac{k_{qb}}{T'_{do}} & -\frac{k_{q\delta b}}{T'_{do}} \\ -\frac{k_A k_{ve}}{T_A} & -\frac{k_A k_{v\delta e}}{T_A} & -\frac{k_A k_{vb}}{T_A} & -\frac{k_A k_{v\delta b}}{T_A} \\ k_{oe} & k_{o\delta e} & k_{ob} & k_{o\delta b} \end{bmatrix} \begin{bmatrix} \Delta m_E \\ \Delta\delta_E \\ \Delta m_B \\ \Delta\delta_B \end{bmatrix} \quad (19)$$

Where Δm_E, Δm_B, $\Delta\delta_E$ and $\Delta\delta_B$ are the deviation of input control signals of the UPFC. Also in this study IEEE Type- ST1A excitation system was used.

IV. CONTROLLER DESIGN

Lead-Lag Controller Design:

As mentioned before, in this study two different controllers have been used to damp LFO. The first one is conventional lead-lag controller. It consists of gain block, washout block, lead-lag compensator block. The washout block is considered as a high-pass filter, with the time constant TW. Without this block steady changes in input would modify the output. The value of TW is not critical and may be in the range of 1 to 20 seconds. In this study, the parameters obtained from lead-lag controller design were used.

Adaptive Neuro-Fuzzy Controller Design:

Another controller is adaptive neuro-fuzzy controller. In this section, we will present the procedure of designing of the adaptive neuro-fuzzy controller. In this research, the neuro fuzzy controller has 2 inputs that are $\Delta\delta$ and $\Delta\omega$ and it has 1 output that is $f \in \{ \Delta m_E, \Delta\delta_E, \Delta m_B, \Delta\delta_B \}$. For each input 20 membership functions and also 20 rules in the rules base is considered. Figure 5 demonstrates the structure of adaptive neuro-fuzzy controller for a sugeno fuzzy model with 2 inputs and 20 rules.

In Figure 9, a Sugeno type of fuzzy system has the rule base with rules such as follows:

1. If $\Delta\delta$ is A_1 and $\Delta\omega$ is B_1 then $f_1=p_1\,\Delta\delta+q_1\,\Delta\omega+r_1$.
2. If $\Delta\delta$ is A_2 and $\Delta\omega$ is B_2 then $f_2=p_2\,\Delta\delta+q_2\,\Delta\omega+r_2$.

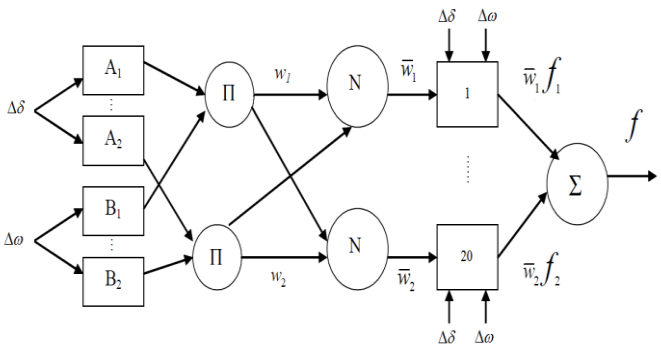

Fig.9. ANFIS architecture for a two-input Sugeno fuzzy model with 20 rules

μ_A and μ_B are the membership functions of fuzzy sets A_i and B_i for i=1,…,20. In evaluating the rules, we choose product for T-norm (logical *and*). Then controller could be designed in following steps:
1. Evaluating the rule premises:

$$w_i = \mu_{A_i}(\Delta\delta)\mu_{B_i}(\Delta\omega), \quad i = 1,\ldots,20. \tag{20}$$

2. Evaluating the implication and the rule consequences:

$$f(\Delta\delta,\Delta\omega) = \frac{w_1(\Delta\delta,\Delta\omega)f_1(\Delta\delta,\Delta\omega)+\ldots+w_{20}(\Delta\delta,\Delta\omega)f_{20}(\Delta\delta,\Delta\omega)}{w_1(\Delta\delta,\Delta\omega)+\ldots+w_{20}(\Delta\delta,\Delta\omega)} \tag{21}$$

Or leaving the arguments out

$$f = \frac{w_1 f_1+\ldots+w_{20}f_{20}}{w_1+\ldots+w_{20}} \tag{22}$$

This can be separated to phases by first defining

$$\overline{w}_i = \frac{w_i}{w_1+\ldots+w_{20}}, \quad i = 1,\ldots,20. \tag{23}$$

These are called normalized firing strengths. Then *f* can be written as

$$f = \overline{w}_1 f_1+\ldots+\overline{w}_{20}f_{20}. \tag{24}$$

The above relation is linear with respect to p_i, q_i, r_i and i=1,…,20. So parameters can be categorized into 2 sets: set of linear parameters and set of nonlinear parameters. Now Hybrid learning algorithm can be applied to obtain values of parameters. Hybrid learning algorithm is combination of linear and nonlinear parameters learning algorithm. This network is called adaptive by Jang and it is functionally equivalent to Sugeno type of a fuzzy system. It is not a unique presentation. With regard to the explanations presented and with the help of MATLAB software, adaptive neuro-fuzzy controller can be designed. The rules surface for designed controller is shown in figure10. One of the advantages of using neuro-fuzzy controller is that we can utilize one of the designed controllers for instance Δm_e controller in place of the other controllers. While if we use conventional lead-lag controller, for each controls parameters, a controller must be designed.

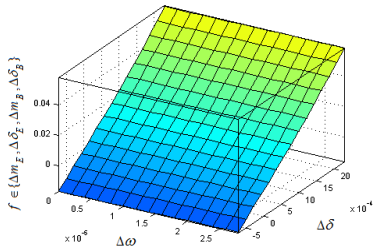

Fig.10. The rules surface

The membership functions for input variable Δω are presented in figure 11.

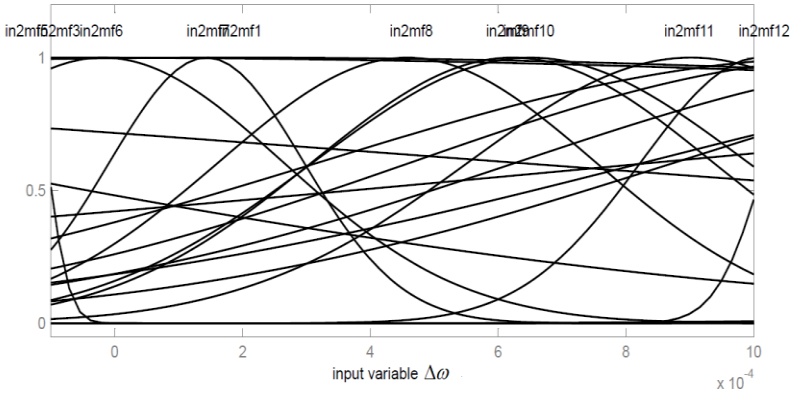

Fig.11 The membership functions for input variable Δω

V. RESULTS

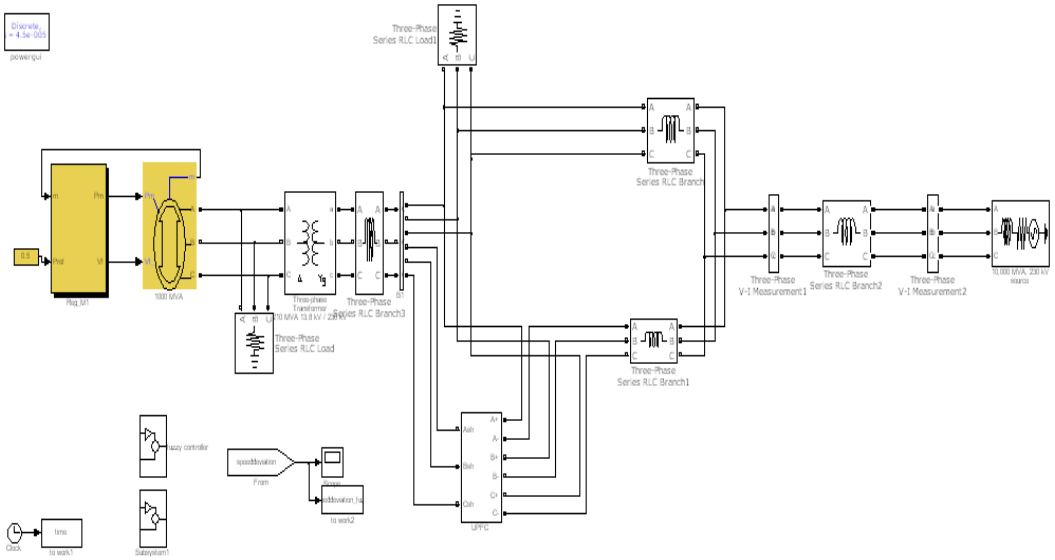

Fig.12 Matlab simulation circuit

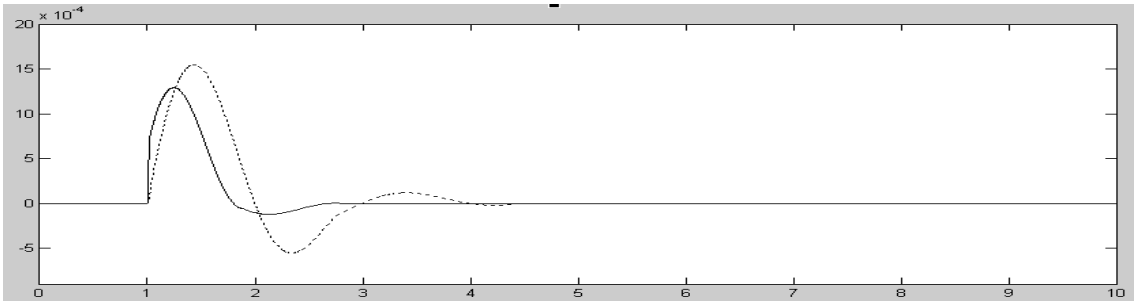

Fig.13 Angular velocity deviation during step change in mechanical input power for nominal load (me Controller)

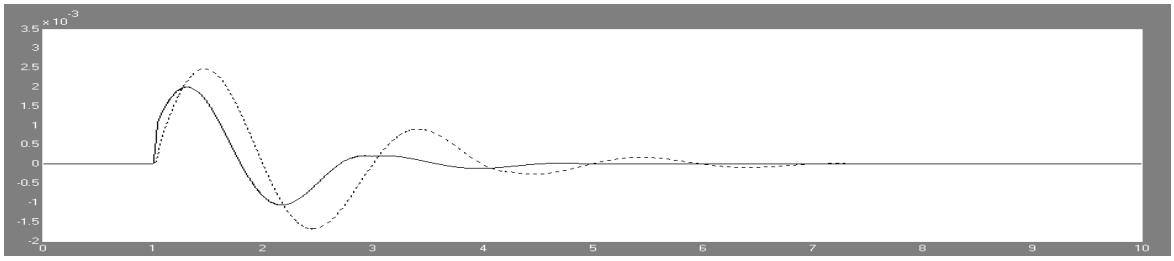

Fig.14 Angular velocity deviation during step change in mechanical input power for light load (me controller)

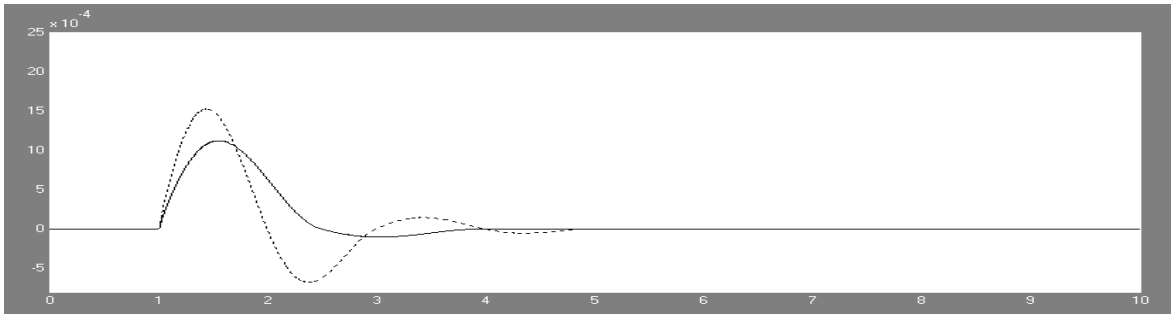

Fig.15 Angular velocity deviation during step change in mechanical input power for nominal load (δe Controller)

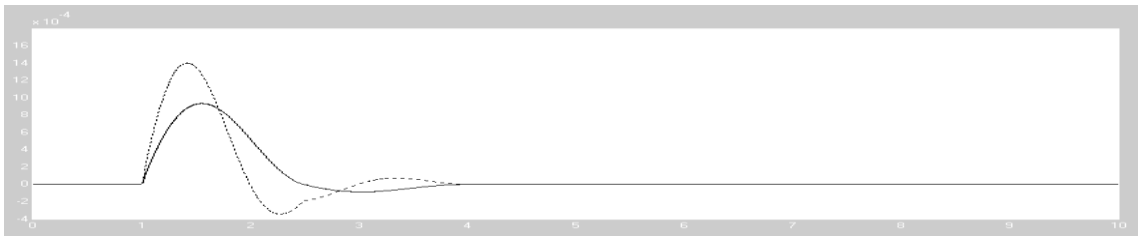

Fig.16 Angular velocity deviation during step change in mechanical input power for nominal load (mb Controller)

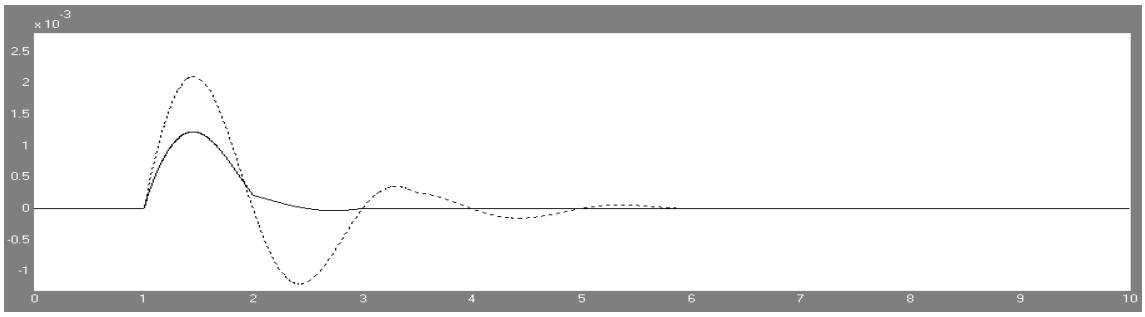

Fig.17 Angular velocity deviation during step change in mechanical input power for nominal load (δb Controller)

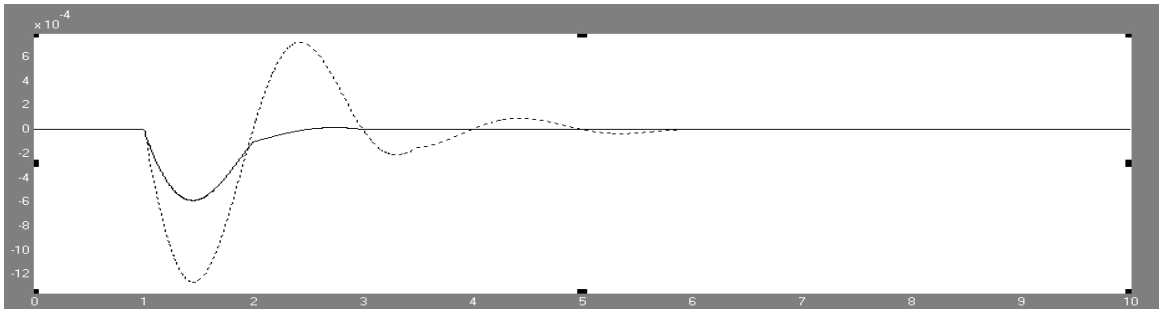

Fig. 18 Response of angular velocity for 5% step change in reference voltage in the case of nominal load (δb Controller)

VI. CONCLUSIONS

With regard to UPFC capability in transient stability improvement and damping LFO of power systems, an adaptive neuro-fuzzy controller for UPFC was presented in this paper. The controller was designed for a single machine infinite bus system. Then simulation results for the system including neuro-fuzzy controller were compared with simulation results for the system including conventional lead-lag controller. Simulations were performed for different kinds of loads. Comparison showed that the proposed adaptive neuro-fuzzy controller has good ability to reduce settling time and reduce amplitude of LFO. Also we can utilize advantages of neural networks such as the ability of adapting to changes, fault tolerance capability, recovery capability, High-speed processing because of parallel processing and ability to build a DSP chip with VLSI Technology.

REFERENCES

[1] N. G. Hingorani and L. Gyugyi, Understanding FACTS: Concepts and Technology of Flexible AC Transmission System, IEEE Press, 2000.

[2] H.F.Wang, F.J.Swift," A Unified Model for the Analysis of FACTS Devices in Damping Power System Oscillations Part I: Single-machine Infinite-bus Power Systems**",** IEEE Transactions on Power Delivery, Vol. 12, No. 2, April 1997, pp.941-946**.**

[3] L. Gyugyi, C.D. Schauder, S.L. Williams, T.R.Rietman, D.R. Torgerson, A. Edris, "The Unified Power Flow Controller: **A** New Approach to Power Transmission Control", IEEE Trans., 1995, pp. 1085-1097.

[4] Wolanki, F. D. Galiana, D. McGillis and G. Joos, "Mid-Point Sitting of FACTS Devices in Transmission Lines," IEEE Transactions on Power Delivery, vol. 12, No. 4, 1997, pp. 1717-1722.

[5] M. Noroozian, L. Angquist, M. Ghandari, and G. Anderson, "Use of UPFC for optimal power flow control", IEEE Trans. on Power Systems, vol. 12, no. 4, 1997, pp. 1629–1634.

[6] A Nabavi-Niaki and M R Iravani. 'Steady-state and Dynamic Models of Unified Power Flow Controller (UPFC) for Power System Studies.' IEEE Transactions on Power Systems, vol 11, 1996, p 1937.
[7] K S Smith, L Ran, J Penman. 'Dynamic Modeling of a Unified Power Flow Controller.' IEE Proceedings-C, vol 144, 1997, pp.7.
[8] H F Wang. 'Damping Function of Unified Power Flow Controller.' IEE Proceedings-C, vol 146, no 1, January 1999, p 81.
[9] H. F. Wang, F. J. Swift, "A Unified Model for the Analysis of FACTS Devices in Damping Power System Oscillations Part I: Single-machine Infinite-bus Power Systems," IEEE Transactions on Power Delivery, Vol. 12, No. 2, April, 1997, pp. 941-946.
[10] P. Kundur,"Power System Stability and Control", McGraw-Hill.

Mr. Gundala Srinivasa Rao[1] *is presently working as Assistant Professor in the department of Electrical & Electronics Engineering at Sri Venkateswara Engineering College, Suryapet. He has 3 years of teaching experience. He obtained master of technology in Power Electronics from Jawaharlal Nehru Technological University, Hyderabad.*

Mr. Venugopal Reddy Bodha[2] was born in India, in 1985.He received the B.Tech degree in Electrical &Electronics Engineering from J.N.T.U, Hyderabad, India, in 2007, And the M.Tech degree in Power Electronics from J.N.T.U, Hyderabad, India, in 2012.He is currently *working as Assistant Professor in the department of Electrical & Electronics Engineering at Sri Venkateswara Engineering College, Suryapet, A.P, India . He has 6 years of teaching experience.*